# Galaxy Clustering Constraints on the Galaxy Size–Halo Connection

Andrew Hearin[1], Peter Behroozi[2], Andrey Kravtsov[3], Benjamin Moster[4]

[1] *Argonne National Laboratory, Argonne, IL, USA 60439, USA*
[2] *Department of Physics, University of Arizona, 1118 E 4th St, Tucson, AZ 85721 USA*
[3] *Department of Astronomy & Astrophysics, The University of Chicago, Chicago, IL 60637 USA*
[4] *Universitäts-Sternwarte, Ludwig-Maximilians-Universität München, Scheinerstr. 1, 81679 München, Germany*

31 August 2017

**ABSTRACT**

We derive empirical modeling constraints on the connection between dark matter halos and the half-mass radius $R_{1/2}$ of galaxy bulges and disks. We show that both $R_{1/2}^{\mathrm{disk}}$ and $R_{1/2}^{\mathrm{bulge}}$ are well-described by power law scaling relations with halo virial radius, $R_{1/2} = AR_{\mathrm{vir}}^{\alpha}$. Novel to this work, we use new SDSS measurements of the $R_{1/2}-$dependence of galaxy clustering to constrain the model parameters, $A_{\mathrm{bulge}}, A_{\mathrm{disk}}, \alpha_{\mathrm{bulge}}, \alpha_{\mathrm{disk}}$, and log-normal scatter $\sigma_{\mathrm{R}_{1/2}}$. Even when only coarsely tuning these parameters to the observed one-point functions $\langle R_{1/2}^{\mathrm{disk}} | M_*^{\mathrm{disk}} \rangle$ and $\langle R_{1/2}^{\mathrm{bulge}} | M_*^{\mathrm{bulge}} \rangle$, our model accurately predicts the observed two-point clustering on small- and large-scales. This success non-trivial, as we show that galaxy clustering is highly sensitive to the physics that shapes satellite galaxy profiles. We find no evidence for the commonly assumed relation between halo spin $\lambda_{\mathrm{halo}}$ and $R_{1/2}^{\mathrm{disk}}$, and show that this assumption cannot be meaningfully constrained with either the clustering or lensing of $L_*$ galaxies. Our results provide simple boundary conditions for more complex and fine-grained models of galaxy size. We make our python code publicly available to support cosmological surveys that require realistic synthetic galaxy populations.

## 1 INTRODUCTION

Some introduction goes here.

## 2 DATA AND SIMULATIONS

### 2.1 Galaxy Sample and Measurements

Our galaxy sample comes from Data Release 10 of the Sloan Digital Sky Survey (SDSS Ahn et al. 2014). We study the same $M_*-$complete galaxy sample used in Behroozi et al. (2015), to which we refer the reader for details. Values for $M_*$ and SFR are taken from the MPA-JHU value-added catalog (Kauffmann et al. 2003; Brinchmann et al. 2004).

We additionally use the catalog of SDSS galaxy profile decompositions provided by Meert et al. (2015). In the version of this catalog that we use, two-dimensional $r-$band profiles were fit with a two-component de Vaucouleurs + exponential profile for the bulge and disk, respectively. We cross-match our DR10 sample against the Meert et al. (2015) scale radius of the composite profile, $R_{1/2}$, and the $r-$band flux ratio of the two components, B/T, giving us a volume-limited galaxy sample with values of $M_*$, sSFR, $R_{1/2}$, and B/T.

We calculate two-point clustering $w_{\mathrm{p}}$ with line-of-sight projection of $\pi_{\max} = 20\mathrm{Mpc}$ using the `correl` program in `UniverseMachine`. Our results in § 4 will give special focus on the dependence of $w_{\mathrm{p}}$ upon composite galaxy size $R_{1/2}$. We will quantify this dependence in terms of *clustering ratios* of "large" vs. "small" galaxies, defined according to whether composite galaxy size is above or below $\langle R_{1/2} | M_* \rangle$, computed as the median of a sliding stellar mass window with a width of $N_{\mathrm{gal}} = 1000$.

Together with the present work, we make publicly available this cross-matched catalog, as well as code to generate the catalog from the original data files and load it into a python interpreter.

### 2.2 Simulation and Halos

`Rockstar` subhalos identified at $z = 0$ in the Bolshoi-Planck simulation are the basis of all our modeling.

### 2.3 Baseline Mock Catalog

#### 2.3.1 Mapping $M_*$ & SFR to halos

The starting point of our model is the best-fit `UniverseMachine` model (Behroozi et al. 2017, in prep).

This model maps stellar mass and star-formation rate to every halo and subhalo at each snapshot in the Bolshoi-Planck simulation. The stellar mass function, quenched fraction, SFR density, and SFR-dependent clustering are all accurately captured by this model from $z = 0 - 10$. The model we have developed in the present work does not depend in an essential way upon the `UniverseMachine` model in particular, we only require some reasonably accurate starting point for the $M_*$ and sSFR values mapped to simulated halos.

### 2.3.2   *Mapping* B/T *to halos*

Our model for galaxy size is further predicated upon the mapping between dark matter halos and B/T, the fraction of stellar mass in the bulge. In a companion paper to this work, we will present a separate empirical model for the B/T−halo connection. For our present purposes, we instead rely upon the simplest possible assumption for this connection that recovers the observed distribution $P(\mathrm{B/T}|M_*, \mathrm{sSFR})$ : we suppose that galaxy B/T has no dependence whatsoever upon halo environment or assembly, beyond what is inherited by the mutual correlation between $M_*$, sSFR and the cosmic web. That is, we map B/T to dark matter halos by using the $M_*$ and sSFR values from `UniverseMachine` to randomly select the B/T of a galaxy from our SDSS sample with a similar $M_*$ and sSFR. The intuitive interpretation of this modeling choice is that we assume the morphology-density relation is entirely determined by the color-density relation.

### 3   GALAXY PROFILE MODEL

Motivated by the Kravtsov (2013) results, we model the half-mass radii of galaxies as separate power law functions of halo virial radius:

$$R_{1/2}^{\mathrm{bulge}} \quad = \quad A_{\mathrm{bulge}} R_{\mathrm{vir}}^{\alpha_{\mathrm{bulge}}} \tag{1}$$

$$R_{1/2}^{\mathrm{disk}} \quad = \quad A_{\mathrm{disk}} R_{\mathrm{vir}}^{\alpha_{\mathrm{disk}}} \tag{2}$$

For central galaxies residing in host halos, we use the present-day virial radius; for satellite galaxies we use the virial radius at the time of accretion, using physical units of kpc. We model the composite size of model galaxies as

$$R_{1/2} = (\mathrm{B/T}) R_{1/2}^{\mathrm{bulge}} + (1 - \mathrm{B/T}) R_{1/2}^{\mathrm{disk}}. \tag{3}$$

When generating Monte Carlo realizations of our model galaxy population, we add log-normal scatter $\sigma_{R_{1/2}}$ separately to each component. Our model for sizes thus has five free parameters: $A_{\mathrm{bulge}}, A_{\mathrm{disk}}, \alpha_{\mathrm{bulge}}, \alpha_{\mathrm{disk}}$, and $\sigma_{R_{1/2}}$.

We reiterate an important distinction drawn in the formulation of our forward modeling approach. In the model described above, $R_{1/2}^{\mathrm{bulge}}$ and $R_{1/2}^{\mathrm{disk}}$ are forward modeling quantities that we aim to constrain through SDSS observations of *composite* galaxy size $R_{1/2}$. In particular, both model and real galaxies will be categorized as "small" or "large" according to whether $R_{1/2}$ is above or below the median size for a galaxy with total stellar mass $M_*$.

### 4   RESULTS

In § 4.1 we show comparisons between the fiducial galaxy profile model described in § 3 and our SDSS sample. We demonstrate the sensitivity of galaxy clustering measurements to the post-infall evolution of satellite profiles in § 4.2, establishing the success of our fiducial model as non-trivial. In § 4.3 we show that even highly idealized measurements of galaxy clustering and lensing are insensitive to assumptions about the relation between $\lambda_{\mathrm{halo}}$ and $R_{1/2}$.

### 4.1   Tests of the Fiducial Power Law Model

The results shown in Kravtsov (2013) simplify our task of parameter space exploration: the assumption that composite galaxy size $R_{1/2}$ scales in linear proportion to halo radius $R_{\mathrm{vir}}$ gives a qualitatively good description of SDSS data over many orders of magnitude in galaxy mass. In Figure 1 we show the scaling of composite galaxy size $R_{1/2}$ with $M_*$, with separate panels dedicated to subsamples of galaxies divided according to value of B/T. We refer to galaxies with B/T < 0.25 as "disk-dominated", B/T >= 0.75 as "bulge-dominated", and 0.25 <= B/T < 0.75 as "mixed morphology".

### 4.2   Sensitivity of Clustering to Satellite Profile Evolution

### 4.3   Insensitivity of Clustering and Lensing to Halo Spin Correlations

### 5   DISCUSSION

### 5.1   Progression from Backwards to Forwards Modeling

### 5.2   Relation to Previous Work

### 6   CONCLUSION

### 6.1   Summary

### REFERENCES

Ahn C. P., Alexandroff R., Allende Prieto C., Anders F., Anderson S. F., Anderton T., Andrews B. H., Aubourg É., Bailey S., Bastien F. A., et al. 2014, ApJS , 211, 17
Behroozi P., Wechsler R., Hearin A., Conroy C., 2017, in prep.
Behroozi P. S., Zhu G., Ferguson H. C., Hearin A. P., Lotz J., Silk J., Kassin S., Lu Y., Croton D., Somerville R. S., Watson D. F., 2015, MNRAS , 450, 1546
Brinchmann J., Charlot S., White S. D. M., Tremonti C., Kauffmann G., Heckman T., Brinkmann J., 2004, MNRAS , 351, 1151
Hearin A. P., Watson D. F., Becker M. R., Reyes R., Berlind A. A., Zentner A. R., 2014, MNRAS , 444, 729
Kauffmann G., Heckman T. M., White S. D. M., et al., 2003, MNRAS , 341, 33
Kravtsov A. V., 2013, ApJL , 764, L31
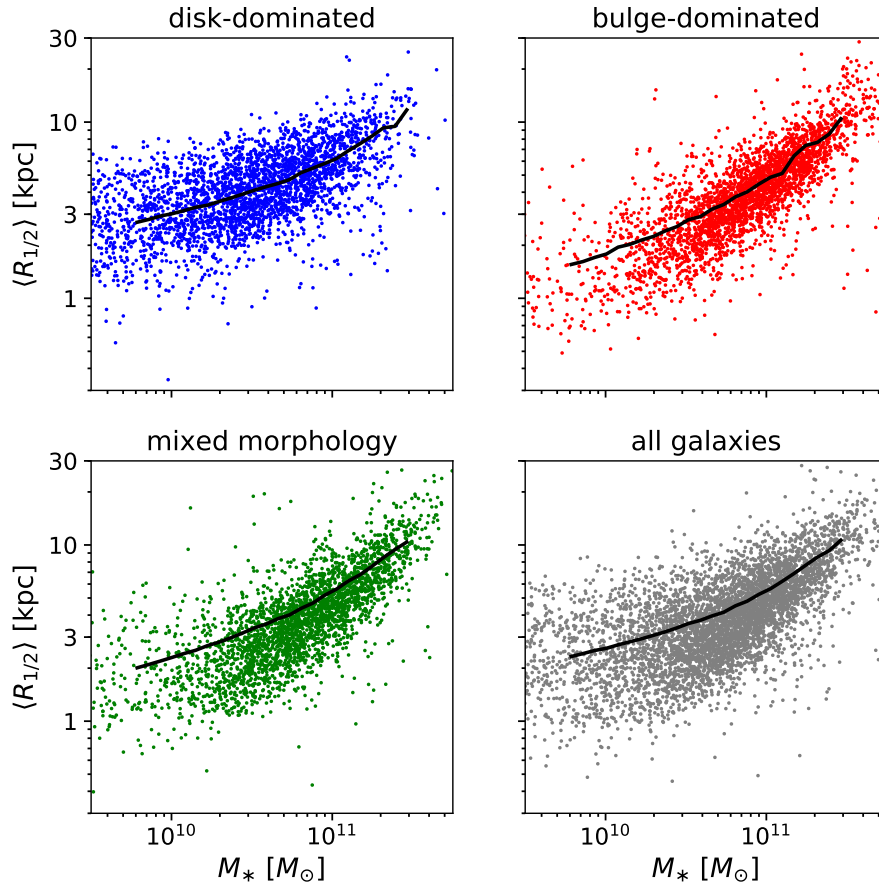Meert A., Vikram V., Bernardi M., 2015, MNRAS , 446, 3943

**Figure 1. One-point data used to fit the fiducial model.** Scattered points show the $R_{1/2} - M_*$ relation for SDSS galaxies as measured in Meert et al. (2015). Bulge-dominated galaxies are defined in terms of the bulge-to-total stellar mass ratio B/T $>= 0.75$, disk-dominated galaxies B/T $< 0.25$, mixed morphology as $0.25 <$ B/T $< 0.75$. The black curve in each panel shows the $R_{1/2} - M_*$ relation implied by our fiducial model, in which $R_{1/2} = AR_{\rm vir}^{\alpha}$, with $A_{\rm disk} = 0.14 = 7A_{\rm bulge}, \alpha_{\rm disk} = 1, \alpha_{\rm bulge} = 5/4$, and uncorrelated log-normal scatter of 0.2 dex about these relations.

Mo H. J., Mao S., White S. D. M., 1998, MNRAS , 295, 319

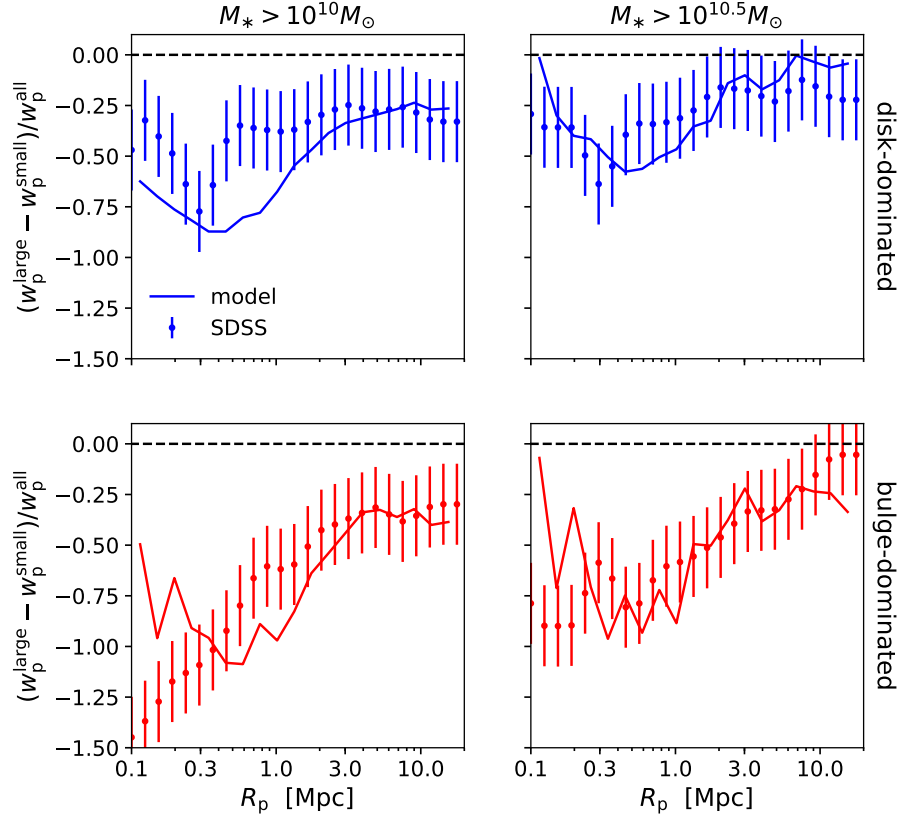Watson D. F., Berlind A. A., Zentner A. R., 2012, ApJ , 754, 90

**Figure 2. Two-point clustering data used to validate the fiducial model.** Points with error bars show new SDSS measurements of the $R_{1/2}$−dependence of projected galaxy clustering, $w_{\mathrm{p}}$, compared to predictions by the model tuned to the measurements shown in Fig. 1. We define a disk or bulge as "large" or "small" according to whether it is above or below the median size for its stellar mass. The y-axis shows clustering strength ratios, so that, for example, a y-axis value of −0.5 corresponds to small galaxies being 50% more strongly clustered than large galaxies of comparable stellar mass. We show results separately for disk-dominated galaxies (*top* panels) and bulge-dominated galaxies (*bottom* panels), and different thresholds in total stellar mass in the *left* and *right* panels. The successful prediction shown here is remarkable because the model was not fit to these data, and because two-point clustering is highly sensitive to the physics that shapes satellite galaxy profiles (see Fig. 4).
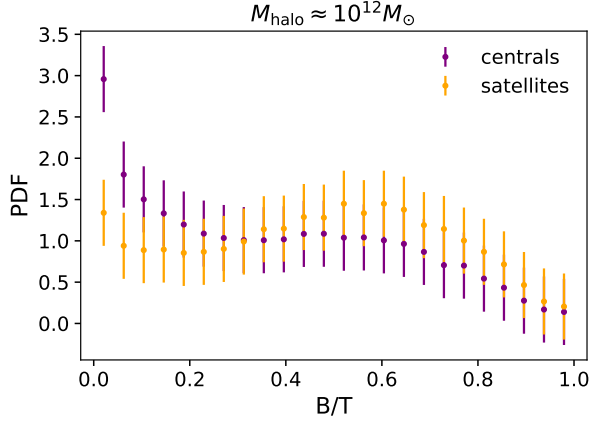
**Figure 3. Morphologies of centrals and satellites of the same halo mass.** We show the PDF of the bulge-to-total stellar mass ratio B/T of central and satellite galaxies of the same halo mass $M_{\mathrm{halo}} = M_{\mathrm{peak}}$. In the model, the PDF of B/T is determined by the stellar mass $M_*$ and specific star-formation rate sSFR statistically determine, with no residual dependence on the cosmic web. Satellite galaxies in the model are "bulgier" than centrals of the same halo mass because satellites are more quiescent than centrals of the same stellar mass. Thus our baseline model ansatz is that the morphology-density relation is purely derived from the color-density relation. Since composite size $R_{1/2}$ in the model is given by $R_{1/2} = (\mathrm{B/T})R_{1/2}^{\mathrm{bulge}} + (1 - \mathrm{B/T})R_{1/2}^{\mathrm{disk}}$, this ansatz in turn implies that smaller galaxies cluster more strongly relative to larger galaxies of the same stellar mass, as seen in the measurements shown in Fig. 2.
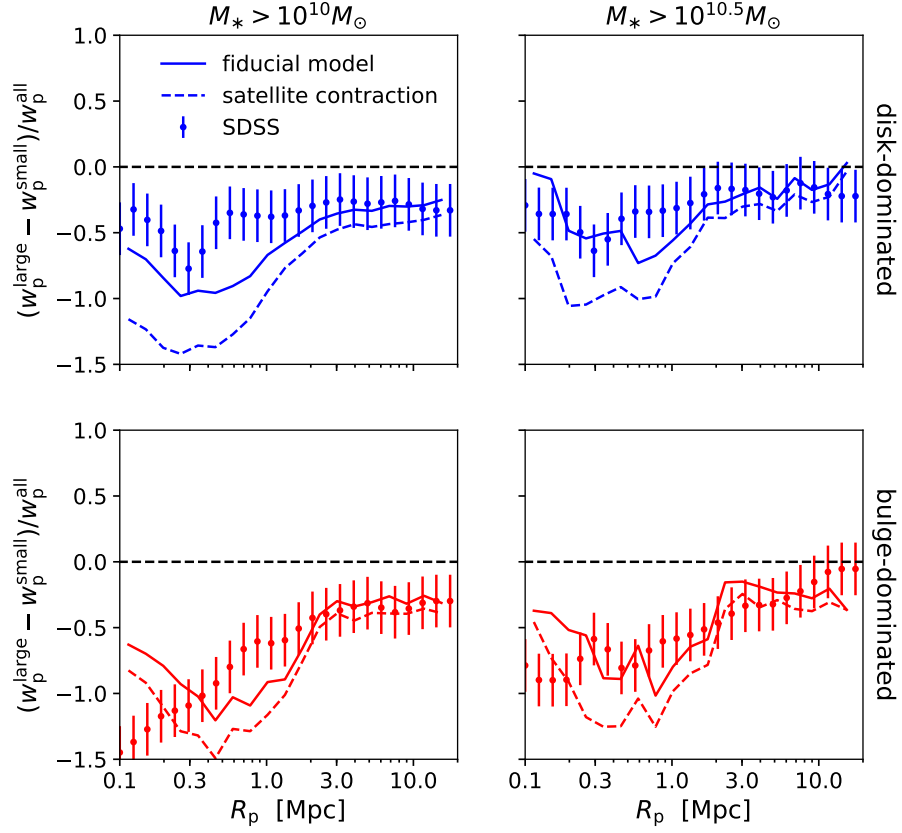
**Figure 4. Clustering provides tight constraints on the relative sizes of centrals and satellites.** Here we compare our fiducial model, in which satellite galaxy size is set by $R_{\rm vir}$ at the time of infall, to an alternative model analogous to Watson et al. (2012) in which satellite sizes contract in proportion to $(M_{\rm vir}/M_{\rm acc})^{1/3}$. The large differences between solid and dashed curves in the top panels show that the $R_{1/2}-$dependence of galaxy clustering ratios is highly sensitive to the post-infall evolution of satellite galaxy profiles. The successful prediction of our fiducial model, in which satellite galaxies neither contract nor puff up after infall, places tight constraints on satellite-specific physical processes, which must be either negligible or conspiratorially produce little-to-no size change after accretion.
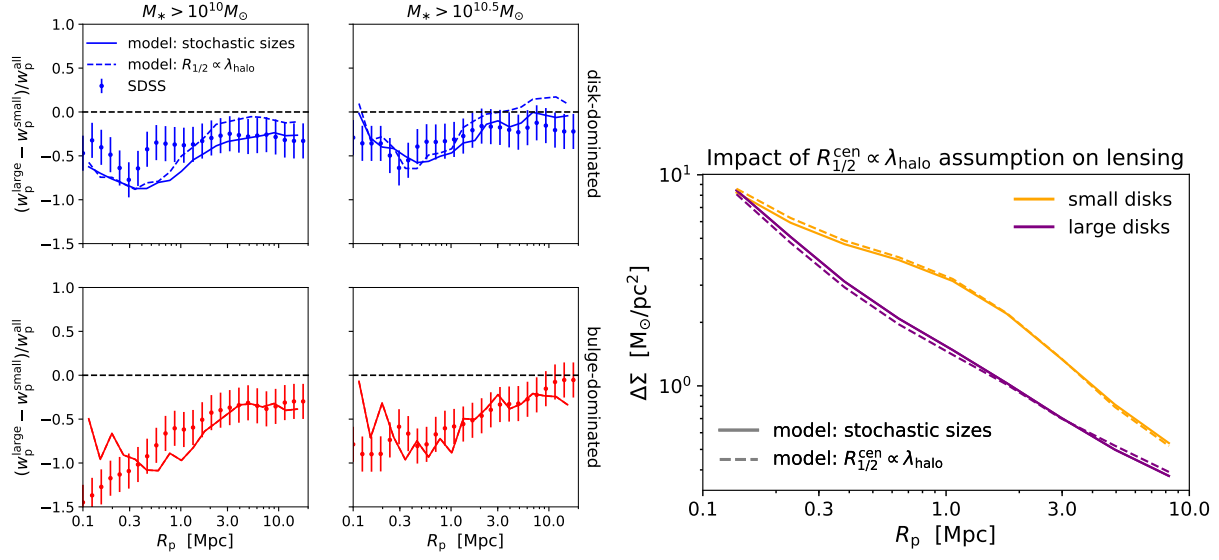
**Figure 5. Clustering and lensing provide no constraining power on the assumption that** $R_{1/2}^{\rm disk} \propto \lambda_{\rm halo}$. We compare the predictions between our fiducial model in which sizes are purely stochastic, and an alternative model motivated by Mo et al. (1998) in which central galaxy disk size is maximally correlated with host halo spin at fixed stellar mass (implemented via conditional abundance matching, e.g., Hearin et al. 2014). The tiny differences between the solid and dashed curves imply that conventional large-scale structure measurements cannot even in principle provide compelling evidence pertaining to the assumption that $R_{1/2}^{\rm disk} \propto \lambda_{\rm halo}$.